Taylor & Francis
Taylor & Francis Group

Journal of Maps

ISSN: (Print) (Online) Journal homepage: https://www.tandfonline.com/loi/tjom20

Linosa island: a unique heritage of Mediterranean biodiversity

Sara Innangi, Luciana Ferraro, Michele Innangi, Gabriella Di Martino, Laura Giordano, Valentina Alice Bracchi & Renato Tonielli

To cite this article: Sara Innangi, Luciana Ferraro, Michele Innangi, Gabriella Di Martino, Laura Giordano, Valentina Alice Bracchi & Renato Tonielli (2024) Linosa island: a unique heritage of Mediterranean biodiversity, Journal of Maps, 20:1, 2297989, DOI: 10.1080/17445647.2023.2297989

To link to this article: https://doi.org/10.1080/17445647.2023.2297989

JOURNAL OF MAPS
2024, VOL. 20, NO. 1, 2297989
https://doi.org/10.1080/17445647.2023.2297989

Linosa island: a unique heritage of Mediterranean biodiversity

Sara Innangi [a*], Luciana Ferraro [a*], Michele Innangi [b], Gabriella Di Martino [a], Laura Giordano [a], Valentina Alice Bracchi [c] and Renato Tonielli [a]

[a]Istituto di Scienze Marine del Consiglio Nazionale delle Ricerche (CNR-ISMAR), Napoli, Italy; [b]Dipartimento di Bioscienze e Territorio, Università degli Studi del Molise, Pesche, Italy; [c]Dipartimento di Scienze dell'Ambiente e della Terra, Università di Milano-Bicocca, Milano, Italy

ABSTRACT

This publication presents a newly created map of the seafloor of Linosa, a volcanic island located in the Sicily Channel (Mediterranean Sea). The seafloor of Linosa was previously surveyed using geophysical and ground-truth data (in 2016 and 2017). Linosa is regarded as a "sentinel area" for alien species and worldwide environmental changes because of its geographical location, making it worthy of particular attention. The predominant habitats found in Linosa have been identified as three priority habitats: Posidonia oceanica meadows, rhodolith beds, and coralligenous habitats, which encompass extensive coral forests. Another crucial environmental indicator is the assemblages of benthic foraminifera, which were previously studied in this area to analyse their correlations with the topography of the seafloor. Hence, all the accessible data was gathered to create a novel comprehensive map of the seabed (at a scale of 1:15,000), with the objective of displaying and highlighting the abundant marine biodiversity of Linosa.

ARTICLE HISTORY
Received 30 June 2023
Revised 11 December 2023
Accepted 15 December 2023

KEYWORDS
Multibeam bathymetry and backscatter; seafloor classification; ground-truth data; rhodolith beds; benthic foraminifera; priority habitat

1. Introduction

The continental shelves of the Mediterranean Sea can be characterized by the occurrence of several habitats of crucial importance for marine biodiversity and conservation, such as the endemic Posidonia oceanica (L.) Delile 1983 meadows, coralligenous and other calcareous bioconcretions (biogenic reefs, maërl and rhodolith beds; Ballesteros, 2006; Barbera et al., 2003; Birkett et al., 1998; Çinar et al., 2020; Dimas et al., 2022; Giakoumi et al., 2013; Martin et al., 2014; Piazzi et al., 2021; UNEP-MAP-RAC, 2008). Posidonia oceanica can be associated with either sedimentary substrates or hardgrounds (i.e. rocky or bio-constructed hard substrates), with the plant rooting in the crevices, and it is widespread throughout the Mediterranean to depths up to 30-40 m in clear water (Pérès & Picard, 1964). In the inner shelf where the depth is greater than maximum limits of P. oceanica, coralligenous assemblages have been found to occur (Ballesteros, 2006). Coralligenous assemblages, together with rhodolith/maërl beds and P. oceanica, have been recognized as VMEs (Vulnerable Marine Ecosystems) by the European Union (EU) and other official environmental commissions (http://www.fao.org/in-action/vulnerable-marine-ecosystems/en/, accessed 20/06/2023; Bensch et al., 2009; Bernal, 2016; Francour et al., 2006; OCEANA, 2009). In addition, these habitats were defined as priority habitats (Habitat Directive 1992/43/EEC), i.e. Class 1120 'Posidonia beds' for P. oceanica meadows, Class 1170 'Reefs' for coralligenous habitat and Class 1110 'Sandbanks which are slightly covered by seawater all the time' for rhodolith/maërl beds (B. Romagnoli et al., 2021). Consequently, the knowledge of their distribution along the continental shelves of the Mediterranean Sea is crucial for the management and conservation of marine resources. Benthic foraminifera, unicellular organisms primarily found in sediments, serve as a significant environmental indicator. They inhabit several microhabitats, including epiphytic, epifaunal, and infaunal, ranging from transitional and marine coastal areas to deep-sea zones. These organisms have been increasingly recognized as reliable ecological indicators for the characterization and monitoring of marine habitats and for the assessment of their ecological status (Sousa et al., 2020). In this context, the Marine Protected Area (MPA) of the Pelagie islands launched a project to assess the conservation status and map the distribution of Posidonia oceanica meadows and coralligenous habitat (Di Martino et al., 2015; Di Martino et al., 2017; Innangi & Tonielli, 2017), also to support the management of the marine ecosystems. In fact, a

CONTACT Michele Innangi michele.innangi@unimol.it
*Sara Innangi and Luciana Ferraro contributed equally to the work.
Supplemental material for this article is available online at https://doi.org/10.1080/17445647.2023.2297989.

basic element for the proper management of MPAs is the classification of the seabed and the recognition of its priority habitats (Bracchi et al., 2017; M. E. Çinar et al., 2020; Ehrhold et al., 2006; Innangi et al., 2019a; Le Bas & Huvenne, 2009; Micallef et al., 2012; Piazzi et al., 2021). Geophysical acoustic data, coupled to ground-truth data obtained with seabed sampling or video images of the seabed, have been more frequently used to map the seafloor to characterize both seagrasses (De Falco et al., 2010; Innangi et al., 2015; Micallef et al., 2012; Tonielli et al., 2016) and coralligenous habitats (Bonacorsi et al., 2012; Bracchi et al., 2015, 2017; De Falco et al., 2022; B. Romagnoli et al., 2021). For this purpose, MultiBeam Echo Sounder (MBES) systems, together with ground-truth data (i.e. Remotely Operated Vehicle ROV investigation, sedimentological and benthic foraminifera samples) have been used to carry out seabed habitat map of Pelagie islands (Innangi et al., 2019a, 2019b, 2022; Tonielli et al., 2016). For the island of Linosa, thanks to the use of oceanographic vessels of the Italian National Research Council (Consiglio Nazionale delle Ricerche CNR), between 2016 and 2017, data were acquired far beyond the boundaries of the marine protected area (MPA), allowing the complete evolution of the submerged volcanic edifice of the island to be observed (C. Romagnoli et al., 2020; Tonielli et al., 2019). The aim of this work is to create a complete map of the seafloor of Linosa, upgrading and integrating the map already published by Innangi et al., 2019a, and to extend it to the depths that have not yet been mapped. The result is a thematic map (scale 1:15,000) of the main sedimentary and benthic environments at depths ranging from 20 to 600 m. The map is enhanced using images obtained from ROVs, which combine the spatial arrangement of benthic foraminifera communities and the identification of species that are representative of various facies types. This provides a comprehensive visualization of the underwater seascape and biodiversity of Linosa.

2. Study area

The Pelagie islands comprise three islands, namely Lampedusa, Linosa, and Lampione. They are situated in the Sicilian Channel (Figure 1a and inset), at approximately 160 km from Sicily, 120 km from Tunisia, and 120 km from Malta (Figure 1a). The Sicilian Channel is a place characterized by a vigorous and fluctuating current system that facilitates the movement of water between the western and eastern Mediterranean basin. More precisely, a large body of Modified Atlantic Mediterranean waters (MAW), which is approximately 200 metres thick, moves towards the east. Upon entering the Sicilian Channel, it splits into two primary streams: the Atlantic Ionian Current (AIS) and the Atlantic Tunisian Current (ATC). The ATC, in particular, flows through the Pelagie islands (Astraldi et al., 2001; Ferraro et al., 2020; Poulain et al., 2012). The intricate flow pattern in the Sicilian Channel, combined with various seabed features like seamounts, banks, volcanoes, pockmarks, and steep-walled basins, play a crucial role in supporting the high biodiversity found in this area. For instance, the presence of these features provides suitable conditions for the growth of healthy deep coral communities and serves as spawning and feeding grounds for several pelagic species, including anchovies, bluefin tuna, and fin whales (UNEP-MAP-RAC, 2015). The Pelagie islands (crossed by the ATC current), are known for their peculiar characteristics of high biodiversity (Innangi et al., 2019b; Maggio et al., 2022; C. Romagnoli et al., 2020; Tonielli et al., 2016) and are included in a MPA (Figure 1b). The intense biological exchange between the main western and eastern sub-basins and migratory activities makes this area a major biodiversity hotspot in the Mediterranean (Corrias et al., 2021; Lo Cascio & Pasta, 2012; Maggio et al., 2022). The sole volcanic island in the archipelago, Linosa, is the focus of this manuscript. Recent research has revealed that its underwater volcanic complex and biodiversity are considerably more extensive than was previously acknowledged (Figure 1b; Innangi et al., 2019a; Tonielli et al., 2019; Ferraro et al., 2020; B. Romagnoli et al., 2021).

3. Methods

3.1. Geophysical data acquisition and processing

Geophysical and sedimentological data were collected by the Institute of Marine Sciences of the National Research Council (ISMAR-CNR) of Naples (Italy) during two oceanographic surveys, 'Linosa 2016' (17-19 August 2016) and 'BioGeoLin 2017' (8-20 September 2017), onboard the R/V Minerva UNO (Innangi et al., 2018). A comprehensive multibeam bathymetric survey was carried out around Linosa Island from depths of around 15 m to 1000 m. This survey achieved nearly entire coverage of the island's underwater slopes, extending all the way to the base of the volcanic structure and its surrounding regions. The survey was performed using a pole-mounted Teledyne SeaBat 7125, 400 kHz MBES, for the shallow water area (for details see Innangi et al., 2019a), whereas the deeper area was investigated using the hull-mounted Teledyne SeaBat 7160, 50 kHz MBES (Tonielli et al., 2019). The technical specifications of the two multibeam systems are summarized in Table 1. The vessel was equipped with a DGPS Fugro SeaStar system that provided a sub-metric positioning accuracy (horizontal 10 cm; vertical 15 cm; for

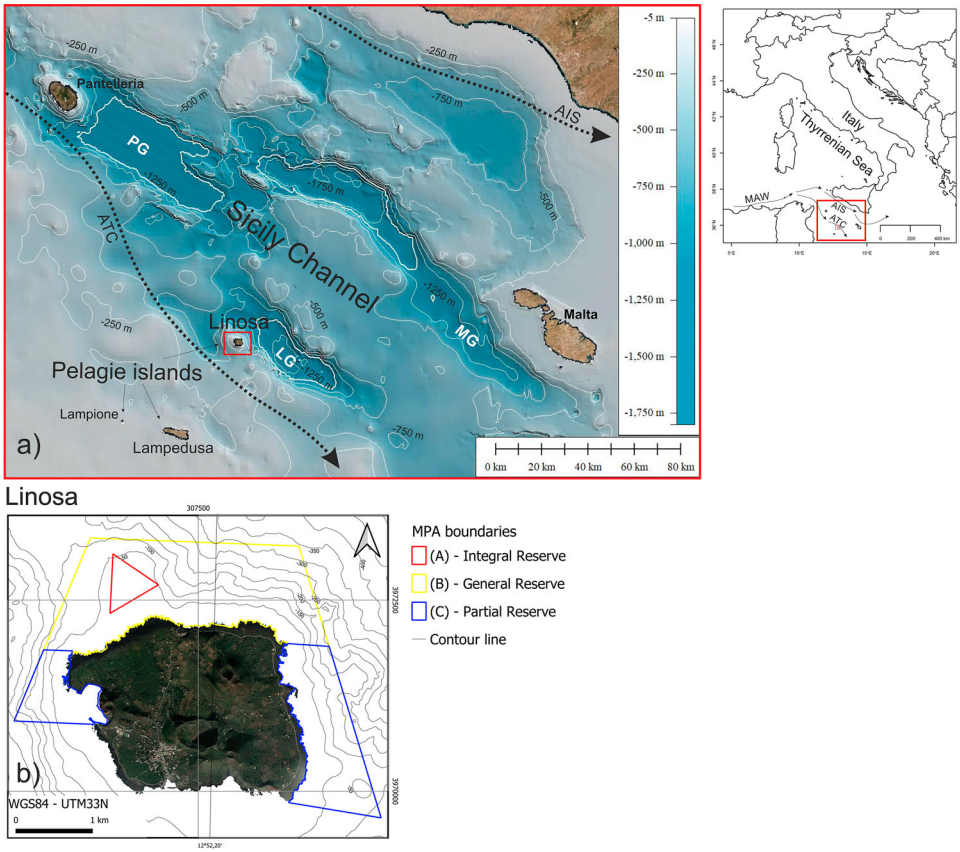

Figure 1. (a) Location map of Linosa Island in the Sicily Channel, central-southern Mediterranean Sea (After Ferraro et al., 2020; Geographic coordinates, Datum WGS84); Marine Digital Terrain Model of Sicily Channel from https://www.emodnet-bathymetry.eu/ (DTM version 2016, date access 12 October 2017). The two principal currents circulation of the Sicily Channel are shown, i.e. the Atlantic Ionian Stream (AIS), the Atlantic Tunisia Current (ATC); b) Linosa island with Marine Protected Area boundaries and relative area restrictions (Projection UTM33N, Datum WGS84).

technical specification see https://media.fugro.com/media/docs/default-source/expertise-docs/our-world/seastar-9205-gnss-receiver-flyer.pdf?sfvrsn = 9ee01f1a_2, accessed 14/06/2022). For both MBES were collected acoustic information through snippet information, i.e. the amplitude time series centred on bottom detection from each beam (De Falco et al., 2010; Hamilton & Parnum, 2011; Innangi et al., 2015; Lurton et al., 2015). Snippet data processing was carried out using FMGeocoder Toolbox (FMGT) in Fledermaus 7.6 version (QPS, 2016), for both MBES systems (for details about processing see Innangi et al., 2019a).

Table 1. Technical Specifications of the two SeaBat, 7125 and 7160 respectively.

Teledyne Seabat 7125	
Frequency	400 kHz
Max ping rate	50 Hz
Along-track trasmit beamwith	1°
Across-track trasmit beamwith	0.5°
Pulse length	30–300 µs – 20 ms Frequency Modulates (X-Range)
Number of beams	512 EA/ED at 400 kHz
Max swath angle	140° in Equi–Distant Mode 165° in Equi–Angle mode
Typical depth	0.5–150 m
Max depth	>175 m at 400 kHz
Depth resolution	6 mm
Teledyne Seabat 7160	
Frequency	44 kHz
Max ping rate	50 Hz
Along-track trasmit beamwith	1.5°
Across-track trasmit beamwith	2° at nadir
Pulse length	30–300 µs Continous Wave 300 µs – 20 ms Frequency Modulates (X-Range)
Number of beams	512 ED/150 EA
Max swath angle	Greater than 4x water depth
Typical depth	3–3000 m
Max depth	3000 m
Depth resolution	12 cm

3.2. Ground-truth data acquisition and processing

During the surveys, both seafloor sampling and direct ROV video observations were carried out using the Dynamic Position (Kongsberg DP0) system to maintain the vessel's position and heading during sampling operation. A total of 14 surface sediment samples were collected using Reineck box corer and Van Veen grab samplers (Figure 2 and 3). Thus, given that the sampling with the box corer assures a minimum of disturbance of the sediment surface and it was previously used for quantitative investigations of the benthic micro- to macrofauna (i.e. Blomqvist et al., 2015; for technical specification about box corer see

https://www.vliz.be/en/reineckboxcorer-en, accessed 06/06/2023), such samples were chosen to study the stratification and distribution of the rhodolith beds (Basso et al., 2016), while Van Veen grab samplers were chosen to complete the sedimentological analysis supporting the backscatter acoustic facies (see Innangi et al., 2019a for details). This is the main reason why the box corer samples were collected along transects, while the grab ones were single points. The seafloor samples were photographed directly on board and their lithological and macroscopic characteristics were reported. For details about grain-size analyses, see Ferraro et al., 2020. Ground-truth data, in form of video observations, were collected by means of the ROV Pollux III, equipped with a positioning system, a depth sensor, a compass and two video cameras, one in high definition and another in low definition. The ROV surveys were carried out along 17 transects set around the island, from about 384 m to 19 m depth areas (Figure 2). To study the benthic habitat of Linosa Island, the video transects were analysed using the belt transect method. This method is widely used for coral reef assessment and is recommended by the Global Coral Reef Monitoring Network (Hill & Wilkinson, 2004). Changes in the composition of the benthic habitat were recorded by tagging along the transects and recording the geographical position and depth. Substrate type and percent coverage of benthic organisms, identified at a coarse taxonomic level, were visually estimated for each sector of the video transect between two tags (B. Romagnoli et al., 2021). Visual estimation was preferred to other standardized methodologies (e.g. random point count) because it preserves higher accuracy while being less time-consuming (Dethier et al., 1993). This paper follows the survey numbering of ROV transects used in Innangi et al. (2019a), later modified for revision in B. Romagnoli et al. (2021).

3.3. Benthic foraminifera data: acquisition and processing

About 50 cm3 of sediments of the box corer and Van Veen grab samples were collected with a tube of 8 cm in diameter from the interval 0-1 cm of the seafloor for the foraminiferal analyses, and treated following the FOBIMO protocol (Schönfeld et al., 2012), to facilitate distinguishing living from dead foraminiferal tests (see Ferraro et al., 2020 for details). Image dataset of benthic foraminifera was acquired from living and dead foraminiferal specimens, from thirteen sampling sites of Figure 2, in a depth range between 50 and 400 m. We selected 19 most representative species for the different bottom substrates, generally, one or two species for sample. Benthic foraminiferal tests were examined and photographed using an optical stereomicroscope (model Zeiss SteREO Discovery V.8) aiming to provide detailed specimens selection and manipulation. Optical images were acquired with a 16× Ocular, S1.0× Objective Plan, and processed via the microscope imaging software Zen Lite (v. 2012 SP1 black edition, 64 bit).

4. Results and discussions

4.1. Geophysical data

All available data (both from 7125 and from 7160 MBES) were merged to create a bathymetric map and an acoustic mosaic of Linosa (10×10 m cell grid

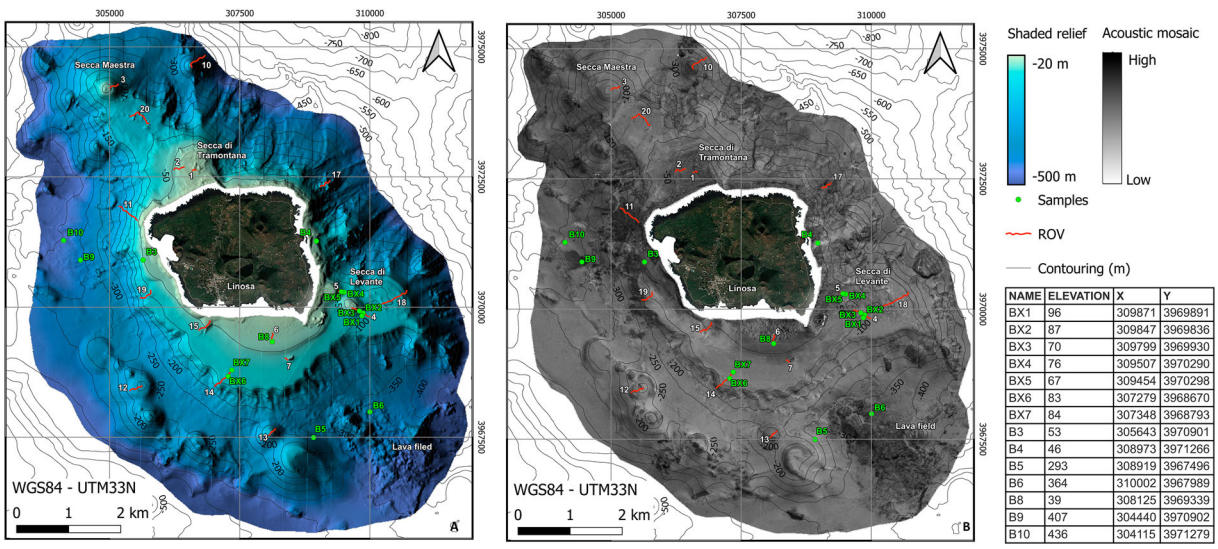

NAME	ELEVATION	X	Y
BX1	96	309871	3969891
BX2	87	309847	3969836
BX3	70	309799	3969930
BX4	76	309507	3970290
BX5	67	309454	3970298
BX6	83	307279	3968670
BX7	84	307348	3968793
B3	53	305643	3970901
B4	46	308973	3971266
B5	293	308919	3967496
B6	364	310002	3967989
B8	39	308125	3969339
B9	407	304440	3970902
B10	436	304115	3971279

Figure 2. Shaded relief (A) and acoustic mosaic (B; 10 m of pixel resolution) of the Linosa bathymetric and backscatter data, respectively, in the depth range of 20-500 m, the extent to which the data on the groundtruth was available. In the legend of acoustic mosaic, the black area corresponds to the highest backscatter, the white area to the lowest.

size; Figure 2). The shaded relief (Figure 2) shows a volcanic edifice mostly extended below sea level and much larger than the small emerged area of the island (Tonielli et al., 2019). The NW sector is characterized by a series of minor submarine eruptive centres, most of which aligned along the volcanic belt, and it is composed of more than 20 individual eruptive centres lying at different depths (C. Romagnoli et al., 2020). Two of these have the summit in relatively shallow water, called 'Secca Maestra' and 'Secca di Tramontana' (Figure 2). The first one is a conical eruptive centre with the top at –38 m, while the second one is a sub-circular morphological volcanic structure that is heavily eroded and is located between 40 and 20 m deep on the insular shelf surface. The whole of the 'Secca di Tramontana' (Figure 1) is included in the Integral MPA Reserve and has been surveyed using ROV instruments (Figure 2) to verify the status of P. oceanica reported in this reserve area. On the opposite side of the island, the southern submarine flank of Linosa is sub-rounded and less deep than the northern flank. It is completely outside the MPA (Figure 1). Several eruptive centres are present on the southern submarine flank of the island, rising from depths between 250 and 570 m and damming small intra-slope basins (C. Romagnoli, 2004). They are roughly arranged in a semi-circular pattern around the island, although local alignments from NNW – SSE to WNW – ESE can be seen in their distribution. On the shelf, the eroded remnants of small eccentric vents are recognized offshore the south-eastern edge of the island. Here two sub-circular truncated cones with diameter around 360/450 m ('Secca di Levante' in Figure 2) rise to a depth of 30/33 m from the shelf surface with flattened summits, characterized by irregular surface. These two volcanic cones are located within the Partial MPA Reserve (Figure 1) and have been surveyed using both ROV and box corer transects (Figure 2) due to the abundant presence of rhodolith beds. Still in the southern submarine sector, yet outside the MPA, previous works (C. Romagnoli, 2004; Tonielli et al., 2019) described the shelf as being covered by volcaniclastic deposits arranged in terraced, prograding depositional bodies. The smoothness of the shelf surface reflects, in fact, the sedimentary coverage, likely fed by reworked volcaniclastic material due to the erosion of pyroclastic and lava units on the island, a process commonly observed in post eruptive, degradational stage of insular volcanoes (Romagnoli & Jakobsson, 2015). On the southeastern flank of the island, between about –300 and –450 m, a lava field is present, giving place to an irregular seabed with relatively fresh morphology (Figure 2A). Finally, the north-eastern submarine flanks of Linosa Island are, instead, characterized by erosive processes, as witnessed by the presence of active canyons with their heads in shallow-water alternating with sub-radial volcanic structures and outcrops, representing the eroded remnants of constructional volcanic features (Chadwick et al., 2005). The acoustic mosaic of the Linosa seafloor was created using a grey scale, with black areas corresponding to higher reflection and white areas to higher absorption (Figure 2B). Although in general the island does not show high variability in terms of acoustic facies, probably due to the nature of volcanic substratum that tends to oversaturate the acoustic signal, and of the overlying deposits, some differences are clearly discernible. For example, the high reflectivity of the lava field due to fresh volcanic material is clearly visible in Figure 2B. It was highlighted that all the most reflective areas correspond to all the areas where the volcanic component prevails over the bioclastic component, even at the same grain size. Furthermore, all areas characterized by continuous and homogeneous coverage of rhodoliths, backscatter tends to stabilize at average values, very similar to those corresponding to the muddy part. Further explanations will be given in section 4.3.

4.2. Ground-truth data

The location of the samples is reported in Figure 2, while the results from Folk Classification are reported in Table 2 (see also Ferraro et al., 2020). Samples varied from gravel (BX4) to mud (B9), although most of the samples were classified as sand (from gravelly sand to sand). More details about the characteristics of samples were reported in Ferraro et al. (2020). The depth of the 17 ROV transects analysed ranged between 19 and 384 m. A detailed analysis of the individual transects was carried out in B. Romagnoli et al. (2021), while in this work a summary and classification were carried out for the creation of the final map. Examples of the video transects analysed are shown in Figure 3 and described in section 4.3. Each transect shows at least one priority habitat (i.e. P. oceanica meadows, coralligenous habitats and rhodoliths) with a total amount of 46% in presence. Coralligenous was the most abundant (24%), followed by rhodoliths (18%) and

Table 2. Folk classification is reported, along with depth (m) of analysed samples.

Sample	Depth	Folk classification
BX1	−96	gravelly Sand
BX2	−100	gravelly Sand
BX3	−71	Sand
BX4	−80	Gravel
BX5	−67	gravelly Sand
BX6	−84	sandy Gravel
BX7	−84	sandy Gravel
B3	−53	Sand
B4	−47	Sand
B5	−297	sandy Mud
B6	−364	gravelly Mud
B8	−39	gravelly Sand
B9	−407	Mud
B10	−440	Mud

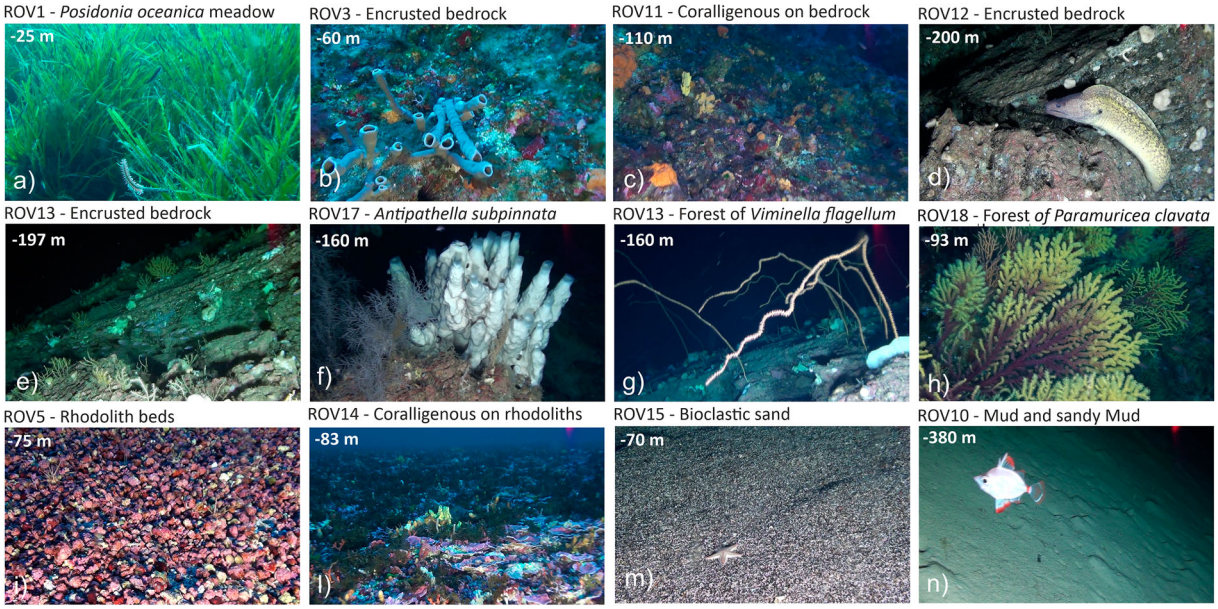

Figure 3. Examples of the video transects analysed. Descriptions on text.

P. oceanica meadows (4%). The remnant can be classified as sand and bedrock, 31% and 16% respectively. Approximately 7% could not be classified due to poor video quality. Table 3 summarizes the percentages of priority habitats observed for each individual ROV (i.e. P. oceanica, coralligenous habitat and rhodolith beds). In addition, because all the bedrock observed for the deeper ROVs are colonized by encrusted organisms, the Encrusted bedrock column was added in Table 3 (see section 4.3), while the column Other contains the percentage of what has been classified as sand, or all that could not be classified.

4.3. Seabed map

A GIS has been implemented with morpho-bathymetric, ground-truth information and ROV image analysis data to support the drafting of a first high-resolution seabed map of Linosa Island, at a scale of 1: 15,000 (Figure 4 and Main Map). A detailed description of the map and legend follows.

4.3.1. B – bedrock

This facies is characterized by a homogeneous pattern of high backscatter, high roughness and variable slope (approximately 20-40 m depth range; Innangi et al., 2019a). B. Romagnoli et al. (2021) indicated macroalgae such as Chlorophyta and Phaeophyta (e.g. Codium bursa and Sargassum sp.). ROV1 and ROV2 were acquired on 'Secca di Tramontana', within the Integral Reserve of the MPA. These showed a rocky substrate, totally covered by P. oceanica meadows in a in a very healthy state (Table 3 and Figure 3a). In some cases, the allochthonous Caulerpa racemosa (J.) Agardh 1973 has also been observed together

Table 3. Summary table of priority habitats, i.e. Posidonia oceanica (referable to priority habitat 1120); Coralligenous habitat (referable to priority habitat 1170); Rhodolith beds (referable to priority habitat 1110). Encrusted bedrock was also reported, while Other includes both sand and no video classification.

ROV	*P. oceanica (%)*	Coralligenous habitat (%)	Rhodolith beds (%)	Encrusted bedrock (%)	Other (%)	From (m)	To (m)
ROV1	91	x	x	x	9	−25	−19
ROV2	33	x	x	x	67	−49	−29
ROV3	x	14	7	x	84	−109	−44
ROV4	x	x	34	x	66	−108	−34
ROV5	x	x	50	x	50	−83	−57
ROV6	57	x	x	x	43	−39	−34
ROV7	x	x	45	x	55	−71	−70
ROV10	x	8	x	29	63	−384	−185
ROV11	x	37	x	39	20	−258	−73
ROV12	x	18	x	31	51	−222	−193
ROV13	x	92	x	x	8	−191	−154
ROV14	x	x	82	11	8	−156	−83
ROV15	5	x	x	x	95	−71	−30
ROV17	x	38	x	23	39	−214	−95
ROV18	x	13	19	7	60	−161	−87
ROV19	x	x	10	31	59	−171	−92
ROV20	x	22	32	35	11	−134	−119

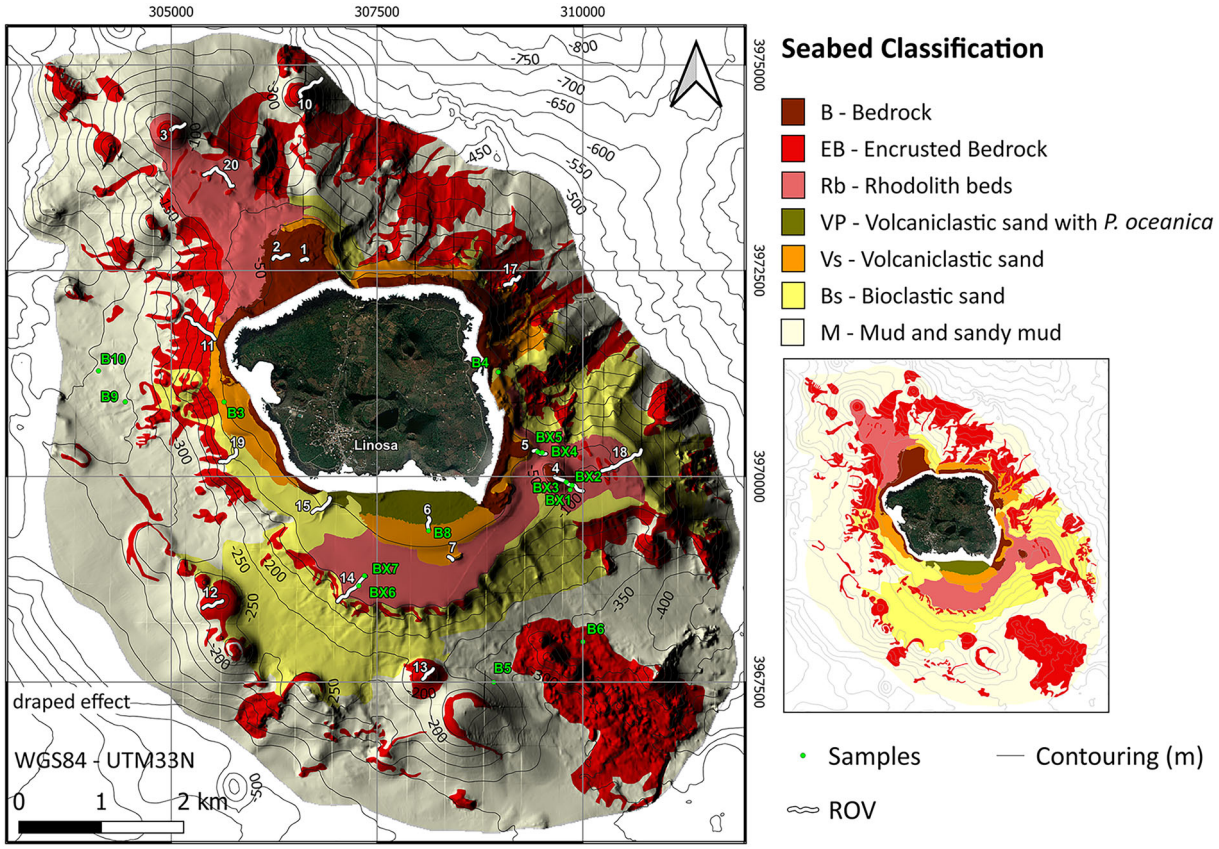

Figure 4. Seabed map of the Linosa island. Descriptions on text.

with P. oceanica (already reported in B. Romagnoli et al. (2021).

4.3.2. EB – encrusted bedrock

High backscatter values at depths ranging from 50 to 300 metres, non-uniform outcrop, and subsurface volcanic bedrock that is frequently colonized by encrusting organisms. It includes also those sectors defined as coralligenous on bedrock in B. Romagnoli et al. (2021), resulting in heterogenous seafloor seascapes. In the ROV analysis, this facies is characterized by a large diversity of encrusting organisms and highly variable environments, but all are united by the presence of the bedrock. For example, the shallowest ROV3 (about – 50 m; Figure 3b and Table 3) was composed of various species of calcareous red and brown algae (such as Rhodophyta and Phaeophyta), with an overlay of encrusting ed erect sponges, bryozoans and anthozoans, identifiable as coralligenous on rocky substrate. The same is for ROV11 (Figure 3c) collected at about 110 m of water depth. While increasing depth, encrusting organisms survive, however the environment is no longer strictly coralligenous (e.g. ROV12 and ROV13 in Figure 3d and Figure 3e, respectively), because of the disappearance of calcareous red algae. On the contrary, some other encrusting organisms appeared, for example black corals, such as Antipathella subpinnata of ROV17 (Figure 3f to 160 m of depth), and the forest of whip corals of Viminella flagellum in ROV13 to about 160 m of depth (Figure 3 g), previously indicated for the Mediterranean Sea from the north-eastern coast of Pantelleria island (Giusti et al., 2012). The ROV18 showed sandy bottom with sparse rhodoliths, and some rocky structures colonized by Paramuricea clavata forests (Figure 3 h), together with massive erect yellow and orange sponges, hydrozoans, bryozoans, and ascidians. At the greatest depth, the bedrock is partially covered by mud, as in the case shown by sampling B6 collected on the lava field, which includes both mud and some coarse volcanic fragments as already reported in B. Romagnoli et al. (2021).

4.3.3. Rb – rhodolith beds

Facies characterized by homogeneous pattern of medium/low backscatter, low roughness, low slope and in a variable depth range of approximately 50–95 metres. They occurred in the southeastern sector of the insular shelf, as shown by ROV14, ROV7, ROV4, ROV5 and ROV18, along with box corer transects (Figure 5). ROV4 and ROV5 were acquired on 'Secca di Levante' within Partial Reserve of MPA and were characterized by dense rhodolith beds that cover bioclastic coarse/medium sand (Figure 3i and Figure 5). Rhodoliths were heterogeneous in size and shape and hosted several species of sponges, small hydrozoans, bryozoans, and ascidians (e.g. Halocynthia sp. and Clavelina sp.), as showed also along ROV14 (Figure 3 l).

Sample	Lithofacies facies	Benthic Foraminifera
BX1 (-96 m)	Rhodolith beds and gravelly sand 	*Miniacina miniacea* (Pallas, 1766) 
BX2 (-100 m)	Rhodolith beds and gravelly sand 	a) *Cyclocibicides vermiculatus* (d'Orbigny, 1826) b) *Asterigerinata mamilla* (Williamson, 1858) 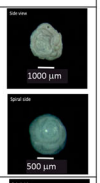
BX3 (-71 m)	Rhodolith beds and bioclastic sand 	a) *Rosalina bradyi* (Cushman, 1915) b) *Planorbulina mediterranensis* (d'Orbigny, 1826) 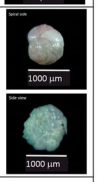
BX4 (-80 m)	Rhodolith beds and gravel 	*Lobatula lobatula* (Walker & Jacob,1798) 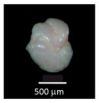
BX5 (-67 m)	Rhodolith beds and gravelly sand 	a) *Elphidium crispum* (Linneo, 1758) 
BX6 (-84 m)	Rhodolith beds and sandy gravel 	a) *Eponides repandus* (Fichtel & Moll) var. concamerata (Williamson, 1858) b) *Spiroloculina excavata* (d'Orbigny 1846) 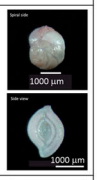
BX7 (-84 m)	Rhodolith beds and sandy gravel 	a) *Sigmoilina costata* Schlumberger, 1893 b) *Triloculina schreiberiana* d'Orbigny, 1839 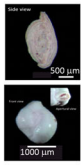

Figure 5. Benthic foraminifera typical of lithological facies for different box corer samples.

Sample	Lithofacies facies	Benthic Foraminifera
B3 (-53 m)	Volcaniclastic sand 	*Peneroplis planatus* (Fichtel & Moll, 1798) 
B4 (-47 m)	Bioclastic sand 	a) *Sorites orbiculus* (Forsskål in Niebuhr, 1775) b) *Peneroplis pertusus* (Forsskål in Niebuhr, 1775) 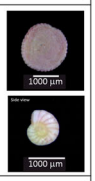
B5 (-29 m)	Sandy mud 	*a) Amphicoryna scalaris* (Batsch, 1791) b) *Lenticulina orbicularis* (d'Orbigny, 1826) 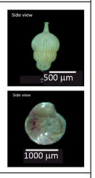
B6 (-364 m)	Gravelly mud 	*Uvigerina mediterranea* (Hofker, 1932) 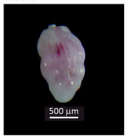
B8 (-39 m)	Volcaniclastic gravelly sand 	*Amphistegina lessonii* (d'Orbigny in Guérin-Méneville, 1832) 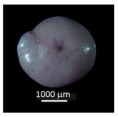
B9 (-407 m)	Mud 	*Melonis pompiloides* (Fichtel & Moll, 1798) 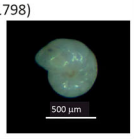

Figure 6. Benthic foraminifera typical of lithological facies for different grab samples.

Phaeophyceae such as Sargassum sp. were also found on these beds, as reported in B. Romagnoli et al. (2021). This facies also characterizes the sector north-west of Linosa, between the 'Secca di Maestra' and the 'Secca di Tramontana', as shown by ROV3 and ROV 20 (Table 3).

4.3.4. VP – volcaniclastic sand with posidonia oceanica

This facies corresponds to a sector with a low slope, and is characterized by the occurrence of seagrass, which is due to an intermediate backscatter and roughness, interrupted by elongated patches of high backscatter. The latter was the seabed, which consists primarily of volcaniclastic coarse sand to pebbles (according to the analysis of sample B8), with scarce bioclastic sand fraction interspersed with rhodoliths (Innangi et al., 2019a). As reported by B. Romagnoli et al. (2021), Caulerpa racemosa was frequently observed on ROV6. This class has only been identified in this sector to the south of the island (Figure 4 and Main Map).

4.3.5. Vs – volcaniclastic sand

Facies characterized by homogeneous high backscatter pattern due to volcaniclastic sand composition, which is more abundant than the bioclastic sand fraction, according with the analysis of sample samples B3 and B8 (Figure 6 and Table 2; Innangi et al., 2019a; Ferraro et al., 2020).

4.3.6. Bs – bioclastic sand

Facies characterized by homogeneous pattern of medium/low backscatter. Seabed composition characterized by bioclastic sand with fewer volcaniclastic sand fractions. The analysis of some samples (e.g. sample B4) and ROVs (e.g. ROV 15 in Figure 3 m) helped

in defining this acoustic facies (Ferraro et al., 2020; Innangi et al., 2019a).

4.3.7. M – mud and sandy mud

The Mud class is characterized by a slightly higher backscatter value than the Bs class, due to the higher compactness and density of the finer particle size class. The samples B5, B9 and B10 made it possible to define these facies (Table 2 and Figure 6; Ferraro et al., 2020) such as the analysis of deeper ROVs, as the ROV 10 in Figure 3n.

4.4. Benthic foraminiferal assemblages

The analysis of foraminiferal assemblages within sediments from areas dominated by different seabed type as Posidonia oceanica meadows, coralligenous, rhodoliths, and sands (volcanic and bioclastic), shows that epiphytic foraminiferal species are very diverse and abundant. The digital image dataset of 19 selected taxa and related lithological facies and sediment texture were reported in Figure 5 and in Figure 6, whereas systematic species descriptions together with species ecology are reported in Appendix A. Sediment textures (Table 2) represent a gradient for distribution of benthic foraminifera from areas particularly dominated by P. oceanica meadows and coralligenous habitat. A total of 140 taxa were identified from the 13 samples that were analysed (Ferraro et al., 2020). The relative abundances of foraminiferal taxa sorted by test material show differences among the 13 samples in the higher abundance of the epiphytic species with calcareous test mainly Asterigerinata, Cyclocibicides, Lobatula, Elphidium, and Eponides, genera which characterize Rhodolith beds that cover bioclastic medium/coarse sand (sites BX1, BX2, BX3, BX4, BX5, BX6 and BX7; Figure 5). In contrast, the most conspicuous taxa which identified the composition across shallowest sites, in areas characterized by volcaniclastic/bioclastic sand (sites B3, B4 and B8), are porcelaneous foraminifera genera as Quinqueloculina and calcareous genera as Peneroplis, Sorites, and Amphistegina (Figure 6). Assemblages from deepest sampling stations (sites B5, B6 and B9), with sediments mainly represented by mud and encrusted bedrock, are mainly dominated by the species Amphicoryna scalaris, Lenticulina orbicularis, Melonis pompiloides, and Uvigerina mediterranea (Figure 6). Benthic assemblage found in Rhodolith beds is dominated by epiphytic species, generally occurring from Posidonia meadows, living attached to the plant's leaves and/or on rhyzomes, such as Asterigerinata mamilla, Lobatula lobatula, Cyclocibicides vermiculatus, Elphidium crispum, Miniacina miniacea, Rosalina bradyi, and Planorbulina mediterranensis (Cimerman & Langer, 1991; Colom, 1974; Jorissen, 1987; Langer, 1988; Sgarrella & Moncharmont Zei, 1993; Figure 5). The benthic foraminiferal assemblage in site BX6 and BX7, still sampled along ROV 14 in the south sector (Figure 4), was mainly represented by the calcareous species Eponides repandus var. concamerata, and by the porcelaneous Spiroloculina xcavate, Sigmoilina costata, and Triloculina schreiberiana. The significative presence of E. repandus var. concamerata, which in the Mediterranean appears to be restricted to the areas characterized by bottom currents and circalittoral detritic substrate (Blanc-Vernet et al., 1979; Ferraro & Molisso, 2000; Sgarrella & Moncharmont Zei, 1993), indicates a high-energy environment with active currents near the bottom. Moreover, miliolid species that characterize these samples, are well represented in the infralittoral and circalittoral zones in the Mediterranean Sea (Sgarrella & Moncharmont Zei, 1993) (Langer, 1993). The benthic foraminiferal assemblage which identifies bioclastic and volcaniclastic sands (site B3, B8 and B4; Figure 6), in the depth range of 46-53 m, is mainly represented by the calcareous species Amphistegina lessonii, Peneroplis pertusus, Peneroplis planatus, and Sorites orbicularis. The genus Peneroplis is made up of species that generally live on bottoms with vegetation covers in the depth-range of 0-50 m (Caruso & Cosentino, 2014; Sgarrella & Moncharmont Zei, 1993). Sorites orbicularis, classified as an 'alien' species in the Mediterranean Sea (Zenetos et al., 2008), is a larger foraminifer which belongs to the group of permanently attached foraminifera, preferentially living on sea grasses and larger algae in the upper photic zone (Langer, 1993). It has been found in the westernmost part of the Palermo and Milazzo gulfs (Caruso et al., 2011; Cosentino et al., 2013) and around the Pelagie islands (Caruso & Cosentino, 2014). Amphistegina is the dominant genus found offshore of the Pelagie Islands, particularly in samples from Linosa island (Caruso & Cosentino, 2014) Amphistegina lessonii has been added to the lists of Mediterranean allochthonous marine organisms (Çinar et al., 2011; Zenetos et al., 2008; Zenetos et al., 2010), while other authors (Caruso & Cosentino, 2014; Langer et al., 2012) consider this species autochthons in the Mediterranean Sea, because it is recolonizing an area which it discontinuously inhabited until 1.3 million years ago. The dominant species occurring on mud sea floors (samples B5, B6 and B9 in Figure 6) were infaunal taxa such as Amphicoryna scalaris, Melonis pompiloides, Uvigerina mediterranea, and Lenticulina orbicularis. These species generally prevail in circalittoral and bathyal mud with variable oxygen conditions (Milker & Schmiedl, 2012; Rögl & Spezzaferri, 2003). L. orbicularis is usually reported from bathyal muds (Blanc-Vernet et al., 1979) and has been identified from middle-outer neritic to above the carbonate compensation depth (CCD; Pezelj et al., 2007; Pezelj et al., 2013).

5. Conclusions

The final seabed map resulting from this work represents a synthesis of all the previous works published around Linosa island with the data acquired during the surveys of the 2016 and 2017, and in particular, all the data collected from three previous research papers (Ferraro et al., 2020; Innangi et al., 2019a; B. Romagnoli et al., 2021). The aim was to standardize information that varies in geographical scales, ranging from the small scale of benthic foraminifera to the intermediate scale of remotely operated vehicles (ROVs), and finally to the large scale of geophysical data. The map of Linosa, as described in Innangi et al., 2019a, was enhanced and updated using data from the ROV study conducted by B. Romagnoli et al., 2021. This was done to account for the higher resolution of the new map compared to the previous version. By incorporating the research conducted by Ferraro et al. in 2020, we have enhanced this mapping by including data on the spatial distribution of benthic foraminiferal assemblages. This comprehensive map presents data on the spatial distribution of coralligenous habitats in the Mediterranean, as well as the size of rhodolite beds and other significant details about priority habitats. It showcases the exceptional biodiversity and distinctive ecological features of this region in a multidisciplinary manner. Furthermore, it is crucial to highlight that the utilization of remotely operated vehicles (ROVs) has facilitated the detection of species that are deemed uncommon. Our findings have further underscored the necessity of expanding the investigation of the profound Mediterranean seabed to accurately recognize and safeguard fragile habitats across their entire distribution.

Software

Bathymetric data were processed with Teledyne PDS2000, as well as the final DTM.

The backscatter data were processed with FMGeocoder Toolbox (FMGT) in QPS Fledermaus 7.6 version.

The Main Map was produced using QGIS version3.28.8-Firenze.

Digital images of benthic foraminifera specimens were acquired and processed via the microscope imaging software Zen Lite (v. 2012 SP1 black edition, 64 bit).

The figures in the text were produced with CorelDRAW 2019.

Acknowledgements

Thanks to the crew of the R/V 'Minerva Uno', for all the support during board and research operations.

We would like to thank the reviewers for their work and for their advice.

Disclosure statement

No potential conflict of interest was reported by the author(s).

Funding

This study benefited from contribution of the project 'Implementation of research activity and monitoring around Pelagie Islands Marine Protected Area', within the project 'CAmBiA – Contabilità Ambientale e Bilancio Ambientale' funded by the Ministry of the Environment and Protection of Land and Sea (MATTM – Ministero dell'Ambiente e della Tutela del Territorio e del Mare), Directive n° 5135 of March 2015. This study also benefited from the contribution of the RITMARE Flagship Project, funded by Ministry of Education, University and Research (MIUR – Ministero dell'Istruzione dell'Università e della Ricerca) [NRP 2011-2013].

Data available statement

All data used to realize the seabed map are property of Consiglio Nazionale delle Ricerche.

Geo-localization information

The map provided area is located at following coordinates: – X min: 311960,371 Y min: 3975464,411 X max: 303011,712 Y max: 3965560,155 (UTM WGS84 zone 33N).

ORCID

Sara Innangi http://orcid.org/0000-0002-7692-9356
Luciana Ferraro http://orcid.org/0000-0002-6491-2274
Michele Innangi http://orcid.org/0000-0003-2362-6025
Gabriella Di Martino http://orcid.org/0000-0001-6630-3432
Laura Giordano http://orcid.org/0000-0003-0390-5297
Valentina Alice Bracchi http://orcid.org/0000-0001-9918-7079
Renato Tonielli http://orcid.org/0000-0002-8792-9511

References

Astraldi, M., Gasparini, G. P., Gervasio, L., & Salusti, E. (2001). Dense Water Dynamics along the Strait of Sicily (Mediterranean Sea). *Journal of Physical Oceanography*, *31*(12), 3457–3475. https://doi.org/10.1175/1520-0485(2001)031<3457:DWDATS>2.0.CO;2

Ballesteros, E. (2006). Mediterranean Coralligenous Assemblages: A Synthesis of Present Knowledge. *Oceanography and Marine Biology*, *44*, 123–195. http://cat.inist.fr/?aModele = afficheN&cpsidt = 17941028

Barbera, C., Bordehore, C., Borg, J. A., Glémarec, M., Grall, J., Hall-Spencer, J. M., De La Huz, C. D., Lanfranco, E., Lastra, M., Moore, P. G., Mora, J., Pita, M. E., Ramos-Esplá, A. A., Rizzo, M., Sánchez-Mata, A., Seva, A., Schembri, P. J., & Valle, C. (2003). Conservation and management of northeast Atlantic and Mediterranean maerl beds. *Aquatic Conservation: Marine and Freshwater Ecosystems*, *13*(SUPPL. 1), 65–76. https://doi.org/10.1002/aqc.569

Basso, D., Babbini, L., Kaleb, S., Bracchi, V. A., & Falace, A. (2016). Monitoring deep Mediterranean rhodolith beds. *Aquatic Conservation: Marine and Freshwater Ecosystems*, *26*(3), 549–561. https://doi.org/10.1002/aqc.2586

Bensch, A., Gianni, M., Greboval, D., Sanders, J., & Hjort, A. (2009). *Worldwide review of bottom fisheries in the high*

seas. FAO. Fisheries Technical Paper, 552(August), 145. http://www.fao.org/docrep/012/i1116e/i1116e00.htm

Bernal, M. (2016). *Management of Deep Sea Fisheries and protection of Vulnerable Marine Ecosystems in the Mediterranean Sea*. The General Fisheries Commission for the Mediterranean, FAO - GFCM Fishery Resources Officer, August.

Birkett, D. A., Maggs, C., & Drig, M. J. (1998). *An overview of dinamics and sensitivity characteristics for conservation management of marine SACs. V*, 1–117.

Blanc-Vernet, L., Clairefond, P., & Orsolini, P. (1979). La mer pélagienne, étude sédimentologique et écologique du Plateau tunisien et du Golfe de Gabès. *Géologie Méditerranéenne*, *6*(1), 171–209. https://doi.org/10.3406/geolm.1979.1081

Blomqvist, S., Ekeroth, N., Elmgren, R., & Hall, P. O. J. (2015). Long overdue improvement of box corer sampling. *Marine Ecology Progress Series*, *538*, 13–21. https://doi.org/10.3354/meps11405

Bonacorsi, M., Pergent-Martini, C., Clabaut, P., & Pergent, G. (2012). Coralligenous "atolls": Discovery of a new morphotype in the Western Mediterranean Sea. *Comptes Rendus - Biologies*, *335*(10–11), 668–672. https://doi.org/10.1016/j.crvi.2012.10.005

Bracchi, V., Basso, D., Marchese, F., Corselli, C., & Savini, A. (2017). Coralligenous morphotypes on subhorizontal substrate: A new categorization. *Continental Shelf Research*, *144*, 10–20. https://doi.org/10.1016/j.csr.2017.06.005

Bracchi, V., Savini, A., Marchese, F., Palamara, S., Basso, D., & Corselli, C. (2015). Coralligenous habitat in the Mediterranean Sea: A geomorphological description from remote data. *Italian Journal of Geosciences*, *134*(1), 32–40. https://doi.org/10.3301/IJG.2014.16

Caruso, A., & Cosentino, C. (2014). The first colonization of the Genus Amphistegina and other exotic benthic foraminifera of the Pelagian Islands and south-eastern Sicily (central Mediterranean Sea). *Marine Micropaleontology*, *111*, 38–52. https://doi.org/10.1016/j.marmicro.2014.05.002

Caruso, A., Cosentino, C., Tranchina, L., & Brai, M. (2011). Response of benthic foraminifera to heavy metal contamination in marine sediments (Sicilian coasts, Mediterranean Sea). *Chemistry and Ecology*, *27*(1), 9–30. https://doi.org/10.1080/02757540.2010.529076

Chadwick, W. W., Embley, R. W., Johnson, P. D., Merle, S. G., Ristau, S., & Bobbitt, A. (2005). The submarine flanks of Anatahan Volcano, commonwealth of the Northern Mariana Islands. *Journal of Volcanology and Geothermal Research*, *146*(1-3 SPEC. ISS.), 8–25. https://doi.org/10.1016/j.jvolgeores.2004.11.032

Cimerman, F., & Langer, M. R. (1991). Mediterranean Foraminifera: Slovenska Akademija Znanosti in Umetnosti. *Academia Scientiarum et Artium Slovenica*, Ljubljana.

Çinar, M. E., Bilecenoglu, M., ÖZTÜRK, B., Katagan, T., Yokes, M., Aysel, V., Dagli, E., Acik, Ş, Ozcan, T., & Erdogan, H. (2011). An updated review of alien species on the coasts of Turkey. *Mediterranean Marine Science*, *12*(2), 257–315.

Çinar, M. E., Féral, J. P., Arvanitidis, C., David, R., Taşkin, E., Sini, M., Dailianis, T., Doğan, A., Gerovasileiou, V., Evcen, A., Chenuil, A., Dağli, E., Aysel, V., Issaris, Y., Bakir, K., Nalmpantı, M., Sartoretto, S., Salomidi, M., Sapouna, A., … Önen, M. (2020). Coralligenous assemblages along their geographical distribution: Testing of concepts and implications for management. *Aquatic Conservation: Marine and Freshwater Ecosystems*, *30*(8), 1578–1594. https://doi.org/10.1002/aqc.3365

Colom, G. (1974). *Foraminíferos ibéricos: introducción al estudio de las especies bentónicas recientes*.

Corrias, V., Filiciotto, F., & Giardina, F. (2021). Sightings of Risso's Dolphin (Grampus griseus) off the Southern Coast of Linosa Island (South-Central Mediterranean Sea). *Mediterranean Marine Science*, *22*(2), 387–392. https://doi.org/10.12681/mms.23648

Cosentino, C., Pepe, F., Scopelliti, G., Calabrò, M., & Caruso, A. (2013). Benthic foraminiferal response to trace element pollution—the case study of the Gulf of Milazzo, NE Sicily (Central Mediterranean Sea). *Environmental Monitoring and Assessment*, *185*(10), 8777–8802. https://doi.org/10.1007/s10661-013-3292-2

De Falco, G., Conforti, A., Brambilla, W., Budillon, F., Ceccherelli, G., De Luca, M., Di Martino, G., Guala, I., Innangi, S., Pascucci, V., Piazzi, L., Pireddu, L., Santonastaso, A., Tonielli, R., & Simeone, S. (2022). Coralligenous banks along the western and northern continental shelf of Sardinia Island (Mediterranean Sea). *Journal of Maps*, *18*(2), 200–209. https://doi.org/10.1080/17445647.2021.2020179.

De Falco, G., Tonielli, R., Di Martino, G., Innangi, S., Simeone, S., & Parnum, I. M. (2010). Relationships between multibeam backscatter, sediment grain size and Posidonia oceanica seagrass distribution. *Continental Shelf Research*, *30*(18), 1941–1950. https://doi.org/10.1016/j.csr.2010.09.006

Dethier, M. N., Graham, E. S., Cohen, S., & Tear, L. M. (1993). Visual versus random-point percent cover estimations: "objective'' is not always better." *Marine Ecology Progress Series*, *96*(1), 93–100. https://doi.org/10.3354/meps096093

Di Martino, G., Innangi, S., Felsani, M., Giardina, F., & Tonielli, R. (2015). *Acquisizione dati morfo-batimetrici: convenzione Isole Pelagie per il monitoraggio della prateria a Posidonia oceanica*. http://eprints.bice.rm.cnr.it/

Di Martino, G., Tonielli, R., Innangi, S., Romagnoli, C., Di Stefano, M., Grasselli, F., Lombardo, C., Parente, F., Raccuglia, P., Romagnoli, B., & Scarpati, V. (2017). *Rapporto di fine Campagna "BioGeoLin."* http://eprints.bice.rm.cnr.it/17164/

Dimas, X., Fakiris, E., Christodoulou, D., Georgiou, N., Geraga, M., Papathanasiou, V., Orfanidis, S., Kotomatas, S., & Papatheodorou, G. (2022). Marine priority habitat mapping in a Mediterranean conservation area (Gyaros, South Aegean) through multi-platform marine remote sensing techniques. *Frontiers in Marine Science*, *9*, 1–19. https://doi.org/10.3389/fmars.2022.953462

Ehrhold, A., Hamon, D., & Guillaumont, B. (2006). The Rebent monitoring network, a spatially integrated, acoustic approach to surveying nearshore macrobenthic habitats: application to the Bay of Concarneau (South Brittany, France). *ICES Journal of Marine Science*, *63*(9), 1604–1615. https://doi.org/10.1016/j.icesjms.2006.06.010

Ferraro, L., Innangi, S., Di Martino, G., Russo, B., Tonielli, R., & Innangi, M. (2020). Seafloor features and benthic foraminifera off Linosa Island (Sicily Channel, southern Mediterranean). *Journal of Marine Systems*, *211*, 103421. https://doi.org/10.1016/j.jmarsys.2020.103421

Ferraro, L., & Molisso, F. (2000). Sedimentological and paleontological features of sea floor sediments of Penta Palummo and Miseno volcanic highs, Gulf od Naples (South-eastern Tyrrhenian Sea). *Atti Della Accademia Nazionale Dei Lincei. Rendiconti. Classe Di Scienze Fisiche, Matematiche e Naturali*, *11*.

Francour, P., Magréau, J. F., Mannoni, A. P., Cottalorda, M. J., & Gratiot, J. (2006). Management guide for Marine Protected Areas of the Mediterranean sea, Permanent Ecological Moorings. Université de Nice-Sophia Antipolis & Parc National de Port-Cros, Nice, 68 pp.

Giakoumi, S., Sini, M., Gerovasileiou, V., Mazor, T., Beher, J., Possingham, H. P., Abdulla, A., Çinar, M. E., Dendrinos, P., Gucu, A. C., Karamanlidis, A. A., Rodic, P., Panayotidis, P., Taskin, E., Jaklin, A., Voultsiadou, E., Webster, C., Zenetos, A., & Katsanevakis, S. (2013). Ecoregion-Based Conservation Planning in the Mediterranean: Dealing with Large-Scale Heterogeneity. *PLoS One*, *8* (10), https://doi.org/10.1371/journal.pone.0076449

Giusti, M., Bo, M., Bavestrello, G., Angiolillo, M., Salvati, E., & Canese, S. (2012). Record of Viminella flagellum (Alcyonacea: Ellisellidae) in Italian waters (Mediterranean Sea). *Marine Biodiversity Records*, *5*, 1–5. https://doi.org/10.1017/S1755267211000510

Hamilton, L. J., & Parnum, I. (2011). Acoustic seabed segmentation from direct statistical clustering of entire multibeam sonar backscatter curves. *Continental Shelf Research*, *31*(2), 138–148. https://doi.org/10.1016/j.csr.2010.12.002

Hill, J., & Wilkinson, C. (2004). Methods for ecological monitoring of coral reefs. *Australian Institute of Marine Science, Townsville, 117*. https://doi.org/10.1017/CBO9781107415324.004.

Innangi, S., Barra, M., Di Martino, G., Parnum, I., Tonielli, R., & Mazzola, S. (2015). Reson SeaBat 8125 backscatter data as a tool for seabed characterization (Central Mediterranean, Southern Italy): Results from different processing approaches. *Applied Acoustics*, *87*, 109–122. https://doi.org/10.1016/j.apacoust.2014.06.014

Innangi, S., Di Martino, G., Romagnoli, C., & Tonielli, R. (2019b). Seabed classification around Lampione islet, Pelagie Islands Marine Protected area, Sicily Channel, Mediterranean Sea. *Journal of Maps*, *15*(2), 153–164. https://doi.org/10.1080/17445647.2019.1567401

Innangi, S., Di Martino, G., Tonielli, R., Innangi, M., & Romagnoli, C. (2018). *Seafloor habitat mapping on the "Pelagie Islands" MPA (Sicily Channel) using Remote Sensing Object Image Analysis supported by multibeam bathymetry and ground-truth data*. 2018 IEEE International Workshop on Metrology for the Sea (MetroSea 2018), 167–172.

Innangi, S., Innangi, M., Di Febbraro, M., Di Martino, G., Sacchi, M., & Tonielli, R. (2022). Continuous, High-Resolution Mapping of Coastal Seafloor Sediment Distribution. *Remote Sensing*, *14* (5), 1268. https://doi.org/10.3390/rs14051268.

Innangi, S., & Tonielli, R. (2017). *Relazione finale della Campagna Oceanografica "Linosa."* http://eprints.bice.rm.cnr.it/

Innangi, S., Tonielli, R., Romagnoli, C., Budillon, F., Di Martino, G., Innangi, M., Laterza, R., Le Bas, T., & Lo Iacono, C. (2019a). Seabed mapping in the Pelagie Islands marine protected area (Sicily Channel, southern Mediterranean) using Remote Sensing Object Based Image Analysis (RSOBIA). *Marine Geophysical Research*, *40*(3), 333–355. https://doi.org/10.1007/s11001-018-9371-6

Jorissen, F. J. (1987). The distribution of benthic foraminifera in the Adriatic Sea. *Marine Micropaleontology*, *12*, 21–48. https://doi.org/10.1016/0377-8398(87)90012-0

Langer, M. R. (1988). Recent epiphytic foraminifera from Vulcano (Mediterranean Sea). *Revue de Paléobiologie*, *8*, 827–832.

Langer, M. R. (1993). Epiphytic foraminifera. *Marine Micropaleontology*, *20*(3), 235–265. https://doi.org/10.1016/0377-8398(93)90035-V

Langer, M. R., Weinmann, A. E., Lötters, S., & Rödder, D. (2012). Strangers" in paradise: modeling the biogeographic range expansion of the foraminifera Amphistegina in the Mediterranean Sea. *The Journal of Foraminiferal Research*, *42*(3), 234–244. https://doi.org/10.2113/gsjfr.42.3.234

Le Bas, T. P., & Huvenne, V. A. I. (2009). Acquisition and processing of backscatter data for habitat mapping – Comparison of multibeam and sidescan systems. *Applied Acoustics*, *70*(10), 1248–1257. https://doi.org/10.1016/j.apacoust.2008.07.010

Lo Cascio, P., & Pasta, S. (2012). Lampione, a paradigmatic case of Mediterranean island biodiversity. *Biodiversity Journal*, *3*(4), 311–330.

Lurton, X., Lamarche, G., Brown, C., Lucieer, V., Rice, G., Schimel, A., & Weber, T. (2015). *Backscatter measurements by seafloor-mapping sonars - Guidelines and Recommendations* (Issue MAY).

Maggio, T., Perzia, P., Pazzini, A., Campagnuolo, S., Falautano, M., Mannino, A. M., Allegra, A., & Castriota, L. (2022). Sneaking into a Hotspot of Biodiversity: Coverage and Integrity of a Rhodolith Bed in the Strait of Sicily (Central Mediterranean Sea). *Journal of Marine Science and Engineering*, *10* (12), 1808. https://doi.org/10.3390/jmse10121808.

Martin, C. S., Giannoulaki, M., De Leo, F., Scardi, M., Salomidi, M., Knitweiss, L., Pace, M. L., Garofalo, G., Gristina, M., Ballesteros, E., Bavestrello, G., Belluscio, A., Cebrian, E., Gerakaris, V., Pergent, G., Pergent-Martini, C., Schembri, P. J., Terribile, K., Rizzo, L., … Fraschetti, S. (2014). Coralligenous and maërl habitats: Predictive modelling to identify their spatial distributions across the Mediterranean Sea. *Scientific Reports*, *4*, 1–9. https://doi.org/10.1038/srep05073

Micallef, A., Le Bas, T. P., Huvenne, V. A. I., Blondel, P., Hühnerbach, V., & Deidun, A. (2012). A multi-method approach for benthic habitat mapping of shallow coastal areas with high-resolution multibeam data. *Continental Shelf Research*, *39*, 14–26. https://doi.org/10.1016/j.csr.2012.03.008

Milker, Y., & Schmiedl, G. (2012). A taxonomic guide to modern benthic shelf foraminifera of the western Mediterranean Sea. *Palaeontologia Electronica*, *15*(2), 1–134.

OCEANA. (2009). Developing a list of Vulnerable Marine Ecosystems. *40th Session of the General Fisheries Commission for the Mediterranean Mediterranean VMEs : Diverse, Fragile Habitats That Support Fisheries*.

Pérès, J. M., & Picard, J. (1964). Nouveau manuel de bionomie benthique de la mer Méditerranée. *Recueil Des Travaux de La Station Marine d'Endoume*, *31*(47), 1–131.

Pezelj, D., Mandic, O., & Coric, S. (2013). Paleoenvironmental dynamics in the southern Pannonian Basin during initial Middle Miocene marine flooding. *Geologica Carpathica*, *64*(1), 81.

Pezelj, Đ, Sremac, J., & Sokač, A. (2007). Palaeoecology of the Late Badenian foraminifera and ostracoda from the SW Central Paratethys (Medvednica Mt., Croatia). *Geologia Croatica*, *60*(2), 139–150. https://doi.org/10.4154/GC.2007.03

Piazzi, L., Gennaro, P., Cecchi, E., Bianchi, C. N., Cinti, M. F., Gatti, G., Guala, I., Morri, C., Sartoretto, F., Serena, F., & Montefalcone, M. (2021). Ecological status of coralligenous assemblages: Ten years of application of the ESCA index from local to wide scale validation. *Ecological Indicators*, *121*, 107077. https://doi.org/10.1016/j.ecolind.2020.107077

Poulain, P.-M., Menna, M., & Mauri, E. (2012). Surface Geostrophic Circulation of the Mediterranean Sea Derived from Drifter and Satellite Altimeter Data. *Journal of Physical Oceanography*, *42*(6), 973–990. https://doi.org/10.1175/JPO-D-11-0159.1

QPS. (2016). *Fledermaus v7.6 Manual*.

Rögl, F., & Spezzaferri, S. (2003). *Foraminiferal paleoecology and biostratigraphy of the Mühlbach section (Gaindorf Formation, lower Badenian), Lower Austria*. Annalen Des Naturhistorischen Museums in Wien. Serie A Für Mineralogie Und Petrographie, Geologie Und Paläontologie, Anthropologie Und Prähistorie, 23–75.

Romagnoli, B., Grasselli, F., Costantini, F., Abbiati, M., Romagnoli, C., Innangi, S., Di Martino, G., & Tonielli, R. (2021). *Evaluating the distribution of priority benthic habitats through a remotely operated vehicle to support conservation measures off Linosa Island (Sicily Channel, Mediterranean Sea)*. Aquatic Conservation: Marine and Freshwater Ecosystems, November 2020, 1–14. https://doi.org/10.1002/aqc.3554

Romagnoli, C. (2004). *Submerged depositional terraces around Linosa Island (Sicily Channel)*. In APAT - Memorie descrittive della Carta Geologica D'Italia (pp. 71–74).

Romagnoli, C., Belvisi, V., Innangi, S., Di Martino, G., & Tonielli, R. (2020). New insights on the evolution of the Linosa volcano (Sicily Channel) from the study of its submarine portions. *Marine Geology*, *419*, Article 106060. https://doi.org/10.1016/j.margeo.2019.106060

Romagnoli, C., & Jakobsson, S. P. (2015). Post-eruptive morphological evolution of island volcanoes: Surtsey as a modern case study. *Geomorphology*, *250*, 384–396. https://doi.org/10.1016/j.geomorph.2015.09.016

Schönfeld, J., Alve, E., Geslin, E., Jorissen, F., Korsun, S., Spezzaferri, S., Abramovich, S., Almogi-Labin, A., du Chatelet, E. A., Barras, C., Bergamin, L., Bicchi, E., Bouchet, V., Cearreta, A., Di Bella, L., Dijkstra, N., Disaro, S. T., Ferraro, L., Frontalini, F., Tsujimoto, A. (2012). The FOBIMO (FOraminiferal BIo-MOnitoring) initiative-Towards a standardised protocol for soft-bottom benthic foraminiferal monitoring studies. *Marine Micropaleontology*, *94–95*, 1–13. https://doi.org/10.1016/j.marmicro.2012.06.001

Sgarrella, F., & Moncharmont Zei, M. (1993). Benthic Foraminifera of the Gulf of Naples (Italy): systematics and autoecology. *Bollettino Della Società Paleontologica Italiana*, *32*(2), 145–264. ISSN 0583-7979.

Sousa, S., Yamashita, C., Semensatto, D., Santarosa, A., Iwai, F., Omachi, C., Disaró, S., Martins, M., Barbosa, C., Bonetti, C. H. C., Vilela, C. G., Laut, L., & Turra, A. (2020). Opportunities and challenges in incorporating benthic foraminifera in marine and coastal environmental biomonitoring of soft sediments: from science to regulation and practice. *Journal of Sedimentary Environments*, *5*(2), 257–265. https://doi.org/10.1007/s43217-020-00011-w

Tonielli, R., Innangi, S., Budillon, F., Di Martino, G., Felsani, M., Giardina, F., Innangi, M., & Filiciotto, F. (2016). Distribution of Posidonia oceanica (L .) Delile meadows around Lampedusa Island (Strait of Sicily, Italy). *Journal of Maps*, *12*(sup1), 249–260. https://doi.org/10.1080/17445647.2016.1195298

Tonielli, R., Innangi, S., Di Martino, G., & Romagnoli, C. (2019). New bathymetry of the Linosa volcanic complex from multibeam systems (Sicily Channel, Mediterranean Sea). *Journal of Maps*, *15*(2), 611–618. https://doi.org/10.1080/17445647.2019.1642807

UNEP-MAP-RAC, S. P. A. (2008). *Action plan for the conservation of the coralligenous and other calcareous bioconcretions in the Mediterranean Sea*. UNEP MAP RAC-SPA Publ., Tunis.

UNEP-MAP-RAC, S. P. A. (2015). United Nations Environment Programme Mediterranean Action Plan. *UNEP MAP RAC-SPA Publ., Tunis*, 29.

Zenetos, A., Gofas, S., Verlaque, M., Çinar, M. E., García Raso, J. E., Bianchi, C. N., Morri, C., Azzurro, E., Bilecenoglu, M., & Froglia, C. (2010). *Alien species in the Mediterranean Sea by 2010. A contribution to the application of European Union's Marine Strategy Framework Directive (MSFD)*. Part I. Spatial distribution.

Zenetos, A., Meric, E., Verlaque, M., Galli, P., Boudouresque, C. F., Giangrande, A., Çinar, M. E., & Bilecenoğlu, M. (2008). Additions to the annotated list of marine alien biota in the Mediterranean with special emphasis on Foraminifera and Parasites. *Mediterranean Marine Science*, *9*(1), 119–166. https://doi.org/10.12681/mms.146